24th INTERNATIONAL CONGRESS ON SOUND AND VIBRATION
23–27 July 2017, London

A STUDY ON SOUND RADIATION FROM A SLAB HIGH-SPEED RAILWAY TRACK SUBJECT TO A FAST-MOVING HARMONIC LOAD

Xiaozhen Sheng, Xinbiao Xiao

State Key Laboratory of Traction Power, Southwest Jiaotong University, Chengdu, Sichuan, 610031, China
Email: shengxiaozhen@hotmail.com

Around 22,000km high-speed railways are in operation in China at maximum speed 300km/h. The main track form is the type of non-ballasted slab track. Although a bogie in a high-speed train generates intensive aero-dynamic noise, rolling noise generated from wheel and track vibrations is still important, even dominant, noise source for both inside and outside the train. Thus, control of rolling noise for high-speed trains running on slab high-speed railway tracks is an important research topic. In this paper, a study is presented on sound radiation from a slab high-speed railway track subject to a fast-moving harmonic load. The track is idealised to be an infinitely long periodic structure with period equal to the length of a slab. The vibrational velocity spectra of the rail and slab are shown to consist of an infinite number of spatially harmonic waves having particular wavenumbers. An acoustic domain is defined to approximate the actual acoustic environment. Sound field generated in the acoustic domain by the track is evaluated by calculating sound radiation from each of the spatially harmonic waves using the two-and-half dimensional acoustic boundary element method. A-weighted sound pressure levels generated by the rail and slab separately are produced for a set of typical track parameters, showing the relative importance of the rail and slab in terms of sound radiation. Effects on rail sound radiation of load speed, load frequency, and acoustic treatment to the slab surface are also investigated.

Keywords: slab railway track, periodic structure, moving load, rolling noise

1. Introduction

For trains running below 250-300km/h, rolling noise generated from wheel and track vibrations is the main railway noise polluting the wayside environment. This, combined with other factors, continuously promotes the importance of rolling noise modelling. Rolling noise modelling has been performed for few decades, mainly in Europe, resulting in few well-known models such as the TWINS [1]. Work are still being carried out to reduce limitations of the models and to improve prediction accuracy [2]. Since ballasted tracks are the main type of railway structure used in Europe, these models have been developed mainly for such a track structure.

China has seen a boom in high-speed railways since 2008. So far around 22,000km high-speed railways are in operation at maximum speed 300km/h. The main track form is the type of non-ballasted slab track. Although a bogie in a high-speed train generates intensive aero-dynamic noise, rolling noise is still an important, even a dominant, noise source for both inside and outside the train [3]. Thus, control of rolling noise for high-speed trains running on slab high-speed railway tracks is an important research topic. However, in contrast to the large number of noise measurements performed in China, rolling noise modelling has not yet received sufficient effort. Published work seems to have too many approximations, e.g. in Ref. [4], the wheel/rail forces are predicted with the train being a multi-rigid body system and sound radiations from the track and moving wheels are dealt with in a very rough way.

As a train travels at high speed along a railway track, each wheel is subject to a wheel/rail force moving at the same speed along its periphery. This fast moving force contains not only a static component, i.e. half the axle load, but also many components of high frequencies generated from wheel-rail interactions. The rotation of the wheel also introduces centrifugal and gyroscopic effects. It is shown in Ref. [5] that the dynamics of a fast rotating wheel is much more complicated than that of a non-, or slowly, rotating wheel, not only affecting wheel/rail interactions, but also affecting sound radiation from the wheel.

On the other hand, the track is an infinitely long periodic structure with period equal to the length of a slab. A slab not only has a much larger radiating area than a sleeper in a ballasted track, it also causes much more effective reflection for sounds radiated from the rails. Thus it can be expected that acoustic characteristics of a non-ballasted slab track will be significantly different from a ballasted track, requiring new efforts for investigation.

In this paper, as a step towards modelling rolling noise for high-speed train operations, a study is presented on sound radiation from a slab high-speed railway track subject to a fast-moving harmonic load. In Section 2, the track model is described and an acoustic domain is defined. The vibrational velocity spectra of the rail and slab are presented in Section 3, together with steps of calculating sound radiations from the rail and slab. In Section 4, A-weighted sound pressure levels generated by the rail and slab separately are produced for a set of typical track parameters, showing the relative importance of the rail and slab in terms of sound radiation. Effects on rail sound radiation of load speed, load frequency and acoustic treatment to the slab surface are also investigated in this Section. The paper is concluded in Section 5.

2. The track model and acoustic domain

2.1 The track model

The slab high-speed railway track is depicted in Fig.1 with a coordinate system shown. The origin of the x-axis is located at the centre of a slab-slab gap. The track consists of rails, rail fastener systems, pre-stressed concrete slabs with cast-in sleepers, a layer of concrete–asphalt (CA) mortar and a concrete base. The concrete base is much stiffer and, for wheel/rail noise modelling, may be approximated to be a rigid foundation. The length of the slab plus the small width of a slab-slab gap is denoted by L. The track structure can be idealised to be an infinitely long periodic structure with period being L. In other words, in every length L, the track repeats all the details present in the interval $[0, L]$, which is termed the 0th bay. The track consists of an infinite number of identical bays, and the jth, where $j = -\infty, \cdots, -1, 0, 1, 2, \cdots + \infty$, bay is located from $x = jL$ to $x = (j+1)L$. Within each bay, there are a number, S, of rail fasteners which connect the rail and the slab. The sth fastener in the jth bay is located at $x = jL + x_s$, where $0 \le x_s < L$.

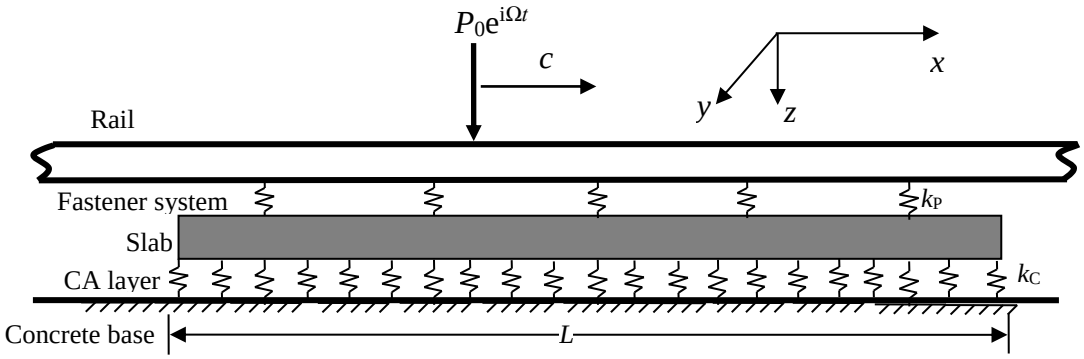

Figure 1: The slab high-speed railway track and coordinate system.

Each rail is subject to a vertical harmonic load of radian frequency Ω moving at speed c along the rail, and the amplitude of the load is denoted by P_0. At $t = 0$, the load is at x_0. Since only vertical track

dynamics is considered in this paper and the dynamics is symmetric about the vertical plane passing the track central line, only half a track has to be modelled, as indicated in Fig.1.

The rail is treated as a Timoshenko beam, and its vibration is defined by $w^R(x, t)$, the vertical displacement of the rail axis and $\psi^R(x, t)$, the rotation angle of the cross-section due to the bending moment only. For slabs, only vertical vibration is important. The dynamics of a slab on the CA layer is described using receptances (displacement divided by force) between positions where fasteners are located. Based on these receptances and the dynamic stiffness of the fasteners, responses of the track to the moving load can be worked out in the form of Fourier transform. For details, see Ref. [6].

2.2 The acoustic domain

Once the vibration of the track is known, sound radiations from the track can be predicted using an appropriate vibro-acoustic prediction method. To do so, an acoustic domain must be first defined.

For a high-speed railway on the ground surface, the acoustic domain may be approximated to be a half-space, as shown in Fig. 2. The horizontal surface beyond the top surface of the slab is assumed to be acoustically hard. Other boundaries of the acoustic domain are radiating, including the top surface of the slabs and the surface of the rails. Connections between a rail and the slabs are ignored, leaving a uniform gap between the rail and the slabs. The effect of the presence of a train on the sound field will not be considered in the current paper (this, however, is important for a train in a tunnel). Thus, the acoustic domain is uniform in the track direction. Fig. 2 also shows the coordinate system for the sound field. The observation point P is defined by radius r and angle θ.

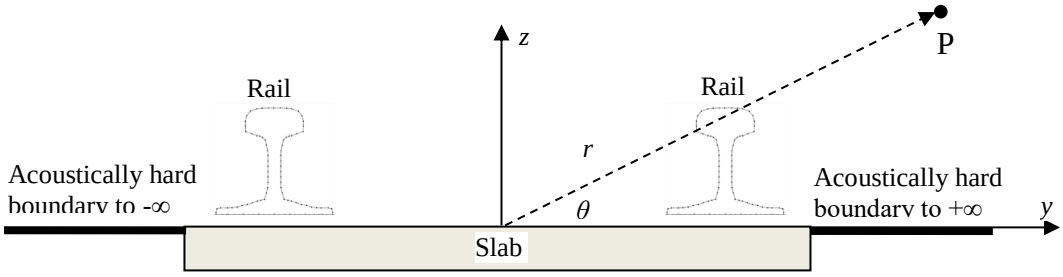

Figure 2: Acoustic domain and coordinate system for sound radiation from the track.

3. Equations for vibro-acoustics of the track

3.1 Equations for calculating vibrations of the track

Observed from the ground, the response of the rail to a moving harmonic load is transient, containing a range of frequency components centred at the load frequency due to structural Doppler Effect. It is shown in Ref. [6] that, the vibrational velocity spectrum of the rail at location x and spectral frequency f, can be expressed as the sum of an infinite number of spatial harmonic waves, i.e.

$$\hat{w}^R(x, f) = \left(\sum_{j=-\infty}^{\infty} g_j \mathrm{e}^{\mathrm{i}\beta_j x} \right) P_0, \ \beta_j = \frac{\Omega - 2\pi f}{c} - \frac{2\pi j}{L} \tag{1}$$

and g_j depends on the track parameters, load speed c, load frequency Ω, spectral frequency f, and all the wavenumbers, β_j defined in Eq. (1).

Similar equation is also developed for the slabs in Ref. [6], as if the slabs were a single beam-like structure of infinite length. In other words, the vibrational velocity spectrum at point (x, y) and spectral frequency f, can also be expressed as the sum of an infinite number of spatial harmonic waves, i.e.

$$\hat{w}^S(x, y, f) = \left(\sum_{j=-\infty}^{\infty} h_j \mathrm{e}^{\mathrm{i}\beta_j x} \right) P_0 . \tag{2}$$

3.2 Steps for calculating sound radiations from the track

For the moving harmonic load, sound pressure perceived at a given position in the acoustic domain is also transient due to acoustic Doppler Effect. Sound pressure at a given location is the sum of that generated from slab vibration and that from rail vibration. These two sound pressure components can and should be computed separately.

3.2.1 Sound generated from slab vibration

For sound generated just from slab vibration, the two rails may be removed to make the acoustic domain simpler. It may be further assumed that vibration variation of the slabs in the lateral direction is negligible, making Eq. (2) independent of *y*. Sound pressure at a given location in the acoustic domain may be produced for a unit slab vibrational velocity defined by

$$\upsilon(x, y, t) = \mathrm{e}^{\mathrm{i}2\pi ft}\mathrm{e}^{-\mathrm{i}\beta x}, \tag{3}$$

for a range of discrete spectral frequencies (f) and wavenumbers (β). This will generate a *Slab Sound Transfer Matrix (SSTM)*. Eq. (3) is a wave component at frequency f and wavenumber β. Sound pressure due to the actual slab vibration given in Eq. (2) can then be easily produced by adding up contributions from all the wave components.

Owning to the fact that the acoustic domain is uniform in the track direction, the sound field induced by the vibrational wave defined in Eq. (3) has the same form as that equation, i.e.

$$p(x, y, z, t) = \tilde{p}(\beta, y, z)\mathrm{e}^{\mathrm{i}2\pi ft}\mathrm{e}^{-\mathrm{i}\beta x}. \tag{4}$$

Since the acoustically hard boundaries of the acoustic domain are infinite in the lateral direction, the slabs are equivalent to an infinitely long (in the *x*-direction) baffled plate. Its sound radiation may be calculated using the following integral equation which is derived from the classic Rayleigh integral equation,

$$\tilde{p}(\beta, y, z) = 2f\rho\mathrm{i}\int_{-0.5b_\mathrm{S}}^{0.5b_\mathrm{S}} K_0(\kappa r)\mathrm{d}y', \tag{5}$$

where, ρ (taken to be 1.21kg/m^3) is air density, b_S is the width of the slab, $K_0(\cdot)$ is the modified Bessel function of the 0th order of the second kind, $r = \sqrt{(y-y')^2 + z^2}$, $\kappa = \sqrt{\beta^2 - k_0^2}$, $k_0 = 2\pi f / c_0$ is the acoustic wavenumber, and c_0 (taken to be 343m/s) is sound speed in air.

3.2.2 Sound generated from rail vibration

For sound radiation from the vibrations of the two rails, the slabs are assumed to be acoustically rigid if no acoustic treatment is made to the slab top surface. When the Timoshenko beam theory is used to describe a rail, the normal velocity of the rail surface can be readily determined if the vibrational velocity of the rail axis is known. Thus, as for the slabs, a *Rail Sound Transfer Matrix (RSTM)* may be produced for a unit vertical vibrational velocity of the rail axis, which is also defined in Eq. (3). The generated sound field can also be described by Eq. (4) of which $\tilde{p}(\beta, y, z)$ can be worked out using the 2.5D acoustic boundary element method [6, 7]. The infinite acoustically hard boundaries in Fig. 2 must be truncated when setting up a 2.5D BEM model. This will cause significant errors in prediction from the model if the lateral dimensions of the model are not sufficiently large. To overcome this difficulty, predictions may be performed for the sources shown in Fig. 3 in the full-space excluding the shadowed strip between the rails.

If acoustic treatment is made to the slabs with a sound absorbing strip laid on the slab top surface, the sound field radiated from the two rails can be calculated using the same model as shown in Fig. 3 with the shadowed strip present between the rails, blocking the rail-slab gap. The surfaces of the strip, together with those of the four rails, construct the boundary of the acoustic domain. Acoustic

impedance is provided to the surface of the strip. An engineering example of such acoustic treatment to the slabs is shown in Fig. 4, and it has negligible influence on wheel/rail force and rail vibration.

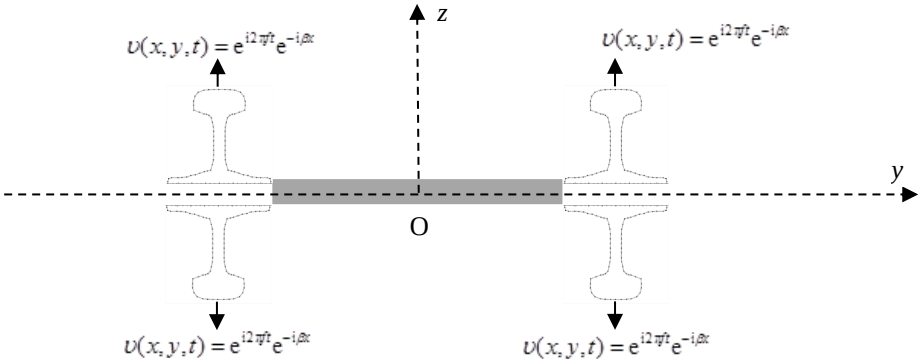

Figure 3: Sources in the full-space generating the same sound field as that by the rails in the half-space.

Figure 4: Acoustic treatment to the slabs (http://www.grout.com.cn/soundabsorption/index.htm).

4. Results

4.1 Track parameters

Parameters typical of the Chinese CRTS II track are listed in Table 1. The railpad stiffness is only 2.5×10^7 N/m in order to protect the slabs. Within each slab, there are $S = 10$ fasteners. In the 0th bay, the x-coordinates of these 10 fasteners are given by $x_s = 0.5L/S + (s-1)d$, where $s = 1, 2, \ldots, 10$.

Table 1: Parameters for the vertical dynamics of the track

Rail/fastener parameters		**Slab parameters**	
Density	$\rho = 7850$ kg/m^3	Period of the track	$L = 6.5$ m
Young's modulus	$E = 2.1\times10^{11}$ N/m^2	Length of the slab	$L_S = 6.45$ m
Shear modulus	$G = 0.81\times10^{11}$ N/m^2	Width of the slab	$b_S = 2.55$ m
Cross-sectional area	$A = 7.69\times10^{-3}$ m^2	Thickness of the slab	$h_S = 0.2$ m
Second moment of area	$I = 30.55\times10^{-6}$ m^4	Young's modulus	$E_S = 3.45\times10^{10}$ N/m^2
Shear coefficient	$\kappa = 0.4$	Poisson ratio	$\nu_S = 0.2$
Vertical rail pad stiffness	$k_P = 2.5\times10^7$ N/m	Density	$\rho_S = 2500$ kg/m^3
Rail pad loss factor	$\eta_P = 0.25$	CA layer stiffness	$k_C = 6.67\times10^9$ N/m^3
Sleeper spacing	$d = 0.65$ m	CA layer loss factor	$\eta_C = 0.1$

4.2 Acoustic property of the slab surface with acoustic treatment

The acoustic property of the slab surface with acoustic treatment is described using impedance z_n which may be approximated by the Delany and Bazley formula [8],

$$z_n' = z_n/(\rho c_0) = 1 + 9.08(1000\,f/\sigma_e)^{-0.75} - 11.9\mathrm{i}(1000\,f/\sigma_e)^{-0.73}, \tag{6}$$

where, σ_e is flow resistivity, of which three values, 3×10^4, 3×10^5 and 3×10^6 Pa·s/m^2, are investigated, as in Ref. [2]. It is seen that as frequency increases, the real part of the normalised impedance approaches 1 and the imaginary part tends to become zero.

The coefficient of sound absorption for a normal incident wave is given by [9]

$$\alpha(0) = \frac{4\,\mathrm{Re}(z_n)\rho c_0}{[\rho_0 c + \mathrm{Re}(z_n)]^2 + [\mathrm{Im}(z_n)]^2}. \tag{7}$$

For the three values of flow resistivity, the sound absorption coefficient is shown in Fig. 5. It is seen that a lower flow resistivity results in a higher sound absorption coefficient.

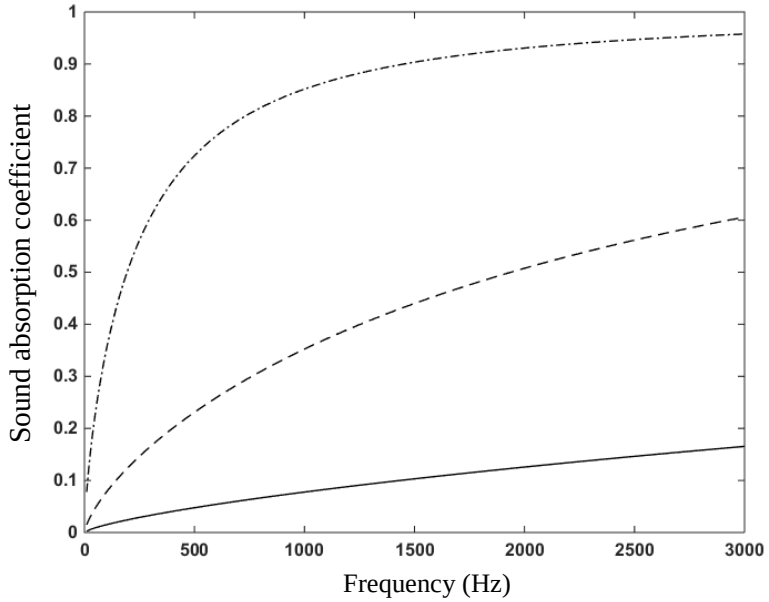

Figure 5: Normal incident sound absorption coefficient. ———, $\sigma_e = 3\times10^6$ Pa·s/m^2; – – –, $\sigma_e = 3\times10^5$ Pa·s/m^2; – · –, $\sigma_e = 3\times10^4$ Pa·s/m^2.

4.3 A-weighted overall sound pressure levels generated by the rails and slabs

Figure 6 shows A-weighted overall (10-3000Hz) sound pressure levels generated from rail vibration (solid lines) and slab vibration (dashed lines) at a ¼ circle of 10m-radius, as function of angle θ (see Fig. 2) (the circle is in the plane with x = 0), for three load frequencies, 200Hz, 500Hz and 1000Hz, and three load speeds, 56m/s (200km/h), 70m/s (250km/h) and 83m/s (300km/h). At t = 0 the load is applied at the mid-span of the rail between the 5th and 6th fasteners of the 0th slab. From Fig. 6 it can be seen that:

(1) For the second and third load frequencies, sound pressure levels due to rail vibration are more than 20dB(A) higher than those due to slab vibration;

(2) However, when the load frequency is 200Hz, the difference in overall sound pressure level between the rail and slab is much smaller, and in particular, when the load speed is 56m/s, sound pressure levels due to slab vibration is higher than that due to rail vibration. And for other two load speeds, this is still true when the angle is less than about 20°;

(3) The dependences of sound radiation from the rails on load frequency and speed are quite complicated. Sound radiation from the rails is strongly affected by load speed but does not always increase with load speed;

(4) There is a trend that sound pressure level increases as observation point moves towards the very top of the slabs where maximum sound pressure occurs;

(5) However, interferences between different sound waves (radiated by the two rails, and reflected by the slabs) are clearly shown as dips and peaks at particular observation locations.

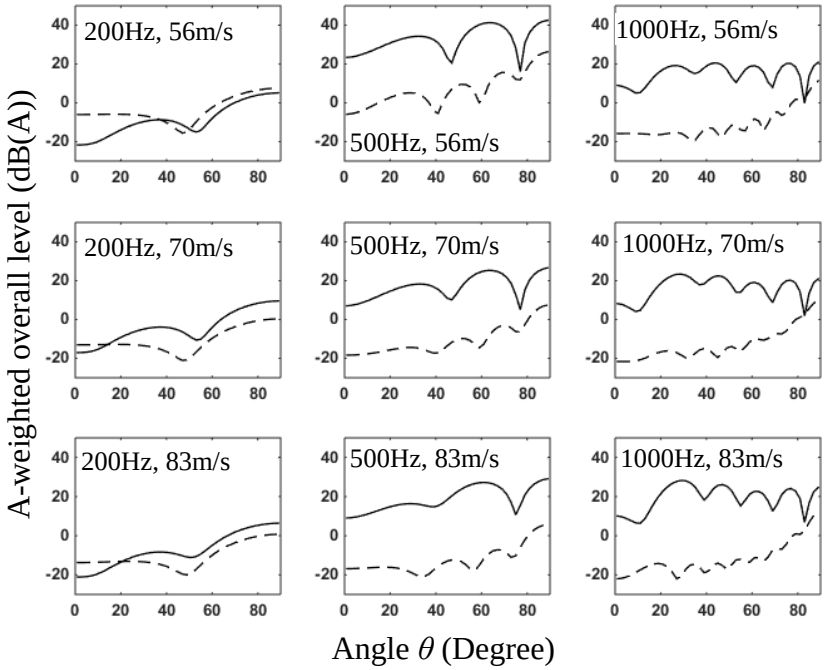

Figure 6: A-weighted overall sound pressure levels produced by rail (——) and slab (– – –) vibrations at a circle of 10m radius due to a unit harmonic load moving along each rail.

4.4 Effect of acoustic treatment to the slabs on sound radiation from the rails

It is shown above that, when load frequency is not too low, sound radiation from the two rails is dominating. To investigate the effect of acoustic treatment to the slabs on rail sound radiation, Fig. 7 shows A-weighted overall sound pressure levels along the same circle as above with (σ_e = 3×10^4 Pa·s/m^2) and without acoustic treatment, for three load frequencies, 500Hz, 1000Hz and 2000Hz, and three load speeds, 56m/s, 70m/s and 83m/s. At t = 0 the load is applied at the mid-span of the rail between the 5th and 6th fasteners of the 0th slab. It can be seen that:

(1) No benefit, and even worse with the acoustic treatment if load frequency is as low as 500Hz. This may be explained to be that the small positive effect of sound absorption of the slab is overcome by the blockage of the rail-slab gaps by the acoustic treatment.

(2) When load frequency is 1000Hz, negative effect is still predicted when the observation angle is less than about 15 °. For other angles, the acoustic treatment reduces noise by few dB(A).

(3) When load frequency is 2000Hz, up to 10dBA noise reduction is predicted for observation angles greater than about 8 °and smaller than about 60 °. For other observation angles, sound pressures are mainly generated by sound waves directly from the two rails.

5. Conclusions

In this paper, a study is presented on sound radiation from a slab high-speed railway track subject to a moving harmonic load. A-weighted sound pressure levels generated by the rail and slab separately are produced for the Chinese CRTS II track. Effects of load speed, load frequency and acoustic treatment to the slab surface are also investigated.

When load frequency is as low as 200Hz, sound from the slab is important compared to the rail, and even exceeds that from the rail when load speed is as low as 56m/s. However, for much higher load frequency, sound radiation from the rail (the slabs behave as a wave reflector) is dominant, although it does not always increase with load speed. Acoustic treatment to the slab is beneficial only when load frequency is high enough, and the observation angle is within a particular range.

Various vibration-controlling slab tracks [10] are used for underground railways but they are normally noisy and noise radiation must be properly addressed. The methodology briefed in this paper can also be applicable. This is issue is still under research.

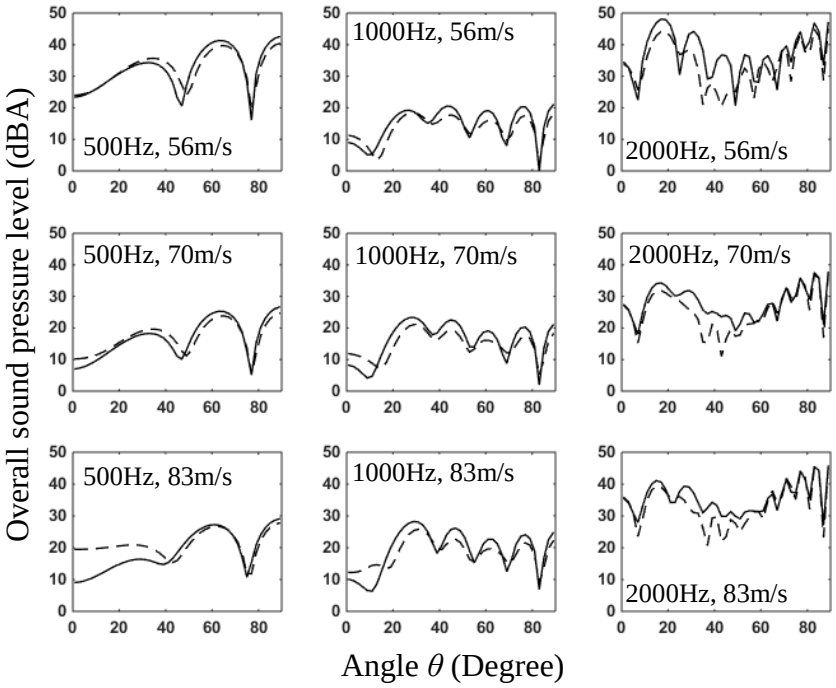

Figure 7: A-weighted overall sound pressure levels produced by the two rails at the circle of 10m-radius due to a unit harmonic load moving along each rail. ——, original slabs; − − −, slabs with $\sigma_e = 3\times10^4$ Pa·s/m^2.

REFERENCES

1 Thompson, D. J., Janssens, M. H. A., *Track Wheel Interaction Noise Software, Version 3.0, Theoretical Manual*, TPD-HAG-MEMO-960343 (1996).

2 Zhang, X., Squicciarini, G., Thompson, D. J., Sound radiation of a railway rail in close proximity to the ground, *Journal of Sound and Vibration*, **362**, 111–124, (2016).

3 Liu, L., Li, Z., Experimental research on the characteristics of Chinese high-speed railway noise source, *Proceedings of the 12th International Workshop on Railway Noise*, Terrigal, Australia, 12–16 September, (2016).

4 Yang, X., Shi, G. The effect of slab track on wheel/rail rolling noise in high-speed railway, *Intelligent Automation & Soft Computing*, **20** (4), 575-585, (2014).

5 Sheng, X., Liu, Y., Zhou, X., The response of a high-speed train wheel to a harmonic wheel-rail force, *Journal of Physics: Conference Series*, **744**, 012145, (2016).

6 Sheng, X., Zhong, T., Li, Y., Vibration and sound radiation of slab high-speed railway track subject to a moving harmonic load, *Journal of Sound and Vibration*, **395**, 160-186, (2017).

7 Nilsson, C. M., Jones, C. J. C., Thompson, D. J., Ryue, J., A waveguide finite element and boundary element approach to calculating the sound radiated by railways and tram rails, *Journal of Sound and Vibration*, **321**, 813-836, (2009).

8 Delany, M. E., Bazley, E. N., Acoustical properties of fibrous absorbent materials, *Applied Acoustics*, **3**, 105-116, (1970).

9 Frank, F., *Foundations of Engineering Acoustics*, Academic Press, (2001).

10 Vogiatzis, K. E., Kouroussis, G., Prediction and efficient control of vibration mitigation using floating slabs: Practical application at Athens metro lines 2 and 3, *International Journal of Rail Transportation*, **3**, 215-232, (2015).